Laser Cooling without Spontaneous Emission

Christopher Corder, Brian Arnold, and Harold Metcalf*
Department of Physics and Astronomy, Stony Brook University, Stony Brook, New York 11794-3800, USA
(Received 25 November 2014; published 28 January 2015)

This Letter reports the demonstration of laser cooling without spontaneous emission, and thereby addresses a significant controversy. It works by restricting the atom-light interaction to a time short compared to a cycle of absorption followed by natural decay. It is achieved by using the bichromatic force on an atomic transition with a relatively long excited state lifetime and a relatively short cooling time so that spontaneous emission effects are minimized. The observed width of the one-dimensional velocity distribution is reduced by ×2 thereby reducing the "temperature" by ×4. Moreover, our results comprise a compression in phase space because the spatial expansion of the atomic sample is limited. This accomplishment is of interest to direct laser cooling of molecules or in experiments where working space or time is limited.

DOI: 10.1103/PhysRevLett.114.043002 PACS numbers: 37.10.De, 37.10.Mn, 37.10.Vz

This Letter describes our experimental demonstration of the controversial notion of laser cooling in the absence of spontaneous emission (SE). It requires a substantial change in how to think about laser cooling. The process is achieved by restricting the atom-light interaction to a time shorter than that required for the cycle of absorption followed by SE, and choosing an atomic transition with a relatively long excited state lifetime $\tau \equiv 1/\gamma$ so that SE effects are minimized.

Laser cooling has been demonstrated with monochromatic light using both radiative and dipole forces [1–4]. In these cases, the various force characteristics of velocity range, spatial range, and force magnitude are limited by the properties of the atoms being cooled, particularly their excited state lifetimes τ and the wavelength of the exciting transition $\lambda \equiv 2\pi/k$. With polychromatic light, these limitations have been overcome by both the bichromatic force [5–7] and adiabatic rapid passage [8–10]. Perhaps the most prominent characteristic of polychromatic forces is their huge magnitude, arising from the use of stimulated emission in place of SE to return atoms to their ground states for rapid, repeated momentum exchanges with the light field.

In laser cooling, only the outgoing light can remove the thermal energy from the atomic sample. In Doppler molasses or atomic beam slowing, this is enabled by using incident light tuned to a frequency ω_ℓ below atomic resonance ω_a in the laboratory frame by an amount $\delta \equiv \omega_\ell - \omega_a < 0$. For atoms traveling opposite to the light beam, their Doppler shifts bring the incident light frequency closer to ω_a and the subsequent force decelerates them.

But their spontaneously emitted fluorescence has frequency $\omega_a > \omega_\ell$ in the lab frame for all directions except the incident one because of the Doppler shifts, thereby mediating a net energy transfer to the light field. In optical molasses, the same description holds for each of the multiple beams. Thus, the angular distribution of SE mediates the energy removal via the Doppler shifts. Even in more elaborate cooling techniques such as polarization gradient cooling, the fluorescence frequency is higher than the absorbed frequency by approximately the light shift difference between the ground state sublevels.

Thus, SE is required for energy dissipation in laser cooling with monochromatic light because stimulated emission would always be at the frequency of the exciting light in both the atomic and laboratory frames, and hence, preclude energy exchange. Of course, in a polychromatic light field, energy can be removed by purely stimulated processes if absorption of the lower frequency light (i.e., red) is followed by stimulated emission into the higher frequency (blue) field.

In the familiar case of monochromatic light, the 4π solid angle of the SE provides so very many states accessible to the system of atoms + light that it seems natural to assume that the entropy loss of the cooled atoms is also dissipated by this light. But the extension of this notion to the claim that SE is therefore required for entropy dissipation is not necessarily correct, and some examples have been explored in Ref. [11]. There are many different kinds of entropy sinks when ground state atoms (pure state) interact with multiple incoming laser beams (pure states) to form a mixed state even with purely stimulated processes [11]. While it is true that monochromatic light cannot cool atoms by stimulated processes only, polychromatic light fields can mediate both energy and entropy exchange.

However, laser cooling requires more than this. In order to be effective, the cooling force must be finite over some velocity range but vanish at other velocities. Thus, atoms would accumulate in the region of velocity space where the force is zero or very small. In Zeeman beam slowing, this region is tunable, in both optical molasses and polarization gradient cooling, it is centered near $v = 0$.

For the bichromatic force, it can be chosen by the frequency separation 2δ between the two fields.

The mechanisms for these cooling forces to vanish are completely different: in beam slowing, the Doppler and Zeeman shifts combine to cause the atoms to drop out of resonance; in optical molasses, the two opposing forces just balance to make zero net force; in polarization gradient cooling, the width of the atomic wave packet exceeds the optical wavelength within the standing waves for velocities below the recoil velocity $\hbar k/M$; and with the bichromatic force, there are nonadiabatic processes that cause the average force to vanish. None of these mechanisms arise directly from SE processes.

The bichromatic force is implemented with two overlapped standing waves equally detuned from atomic resonance by $\pm\delta$. The magnitude F_B of the bichromatic force depends on the choice of δ, the Rabi frequency Ω, the spatial phase difference of the standing waves, and is weakly velocity dependent over a velocity range $\pm\Delta v_B$ [5,7].

It is instructive to consider the bichromatic force in the modified dressed atom picture. The presence of the two frequencies changes the familiar doublet structure of the dressed state eigenvalues to a huge manifold of states separated by $\hbar\delta$ that was first described in Ref. [12] and extended in Ref. [7]. Because the light field is comprised of standing waves whose intensity varies in space from nodes to antinodes, these eigenvalues oscillate as shown in Fig. 1(a) for the light fields of Fig. 1(b). This is very different from the usual single-frequency, dressed-atom picture because here absorption of one frequency, followed by stimulated emission into the other one, can be repeated, thereby exchanging energy multiple times.

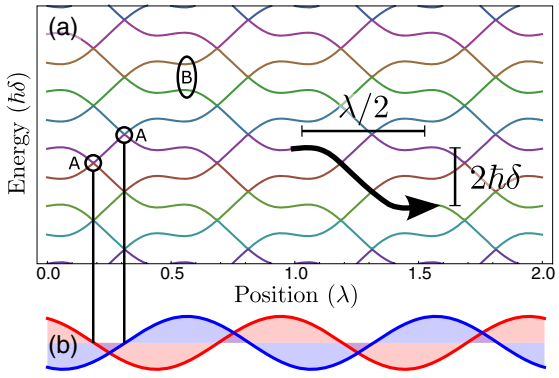

FIG. 1 (color online). Part (a) shows the eigenvalues of the two-frequency dressed state system separated by $\hbar\delta$ where the two fields have equal strength, along with a typical path followed by an atom moving to the right. Circled transition points of the type marked "A" are exact crossings because they occur at the nodes of the standing wave fields shown in part (b). For our case, this occurs for a spatial phase offset of $\lambda/8$ and $\Omega = \sqrt{3/2}\delta$. Point "$B$" in the vertical ellipse marks the location of a possible Landau-Zener transition.

In this picture, the bichromatic force arises from transitions of moving atoms among these manifolds at the crossings between eigenstates of the dressed atom system as indicated by the small circles labeled "A" in Fig. 1(a). These are exact crossings because they occur between states coupled by one field at the nodal points of the other field (see vertical lines in Fig. 1). Thus, moving atoms follow the path indicated by the heavy curved arrow of Fig. 1(a) so the force is

$$F_B = -\frac{\langle \Delta E \rangle}{\Delta z} = \frac{2\hbar\delta}{\lambda/2} = \frac{2\hbar k\delta}{\pi}. \tag{1}$$

When atoms are accelerated to velocities near $v = \pm\Delta v_B$, the magnitude of the force diminishes sharply because of Landau-Zener transitions between the atomic dressed states. This is the point where atomic motional entropy is transferred to the laser fields while both remain part of the "system" [11]. These occur near anticrossings of the type indicated by the vertical ellipse labeled "B" in Fig. 1(a) [7] and the atomic velocities then remain approximately constant. Thus, the final velocity distribution will be peaked near $\pm\Delta v_B \approx \pm\delta/2k$ [7]. Thus, both F_B and Δv_B scale with the value of δ.

Atoms within the velocity range $\pm\Delta v_B$ experience approximately the same uniform force F_B in a selectable direction. They will be accelerated to Δv_B in a characteristic "cooling time"

$$t_c = \frac{2M\Delta v_B}{F_B} = \frac{\pi}{4\omega_r}, \tag{2}$$

where $\omega_r \equiv \hbar k^2/2M$ is the recoil frequency. Even though the atoms have been accelerated to $\pm\Delta v_B \neq 0$, there is still cooling because the final temperature is determined by the width of the velocity distribution. If this distribution has been narrowed, then the atomic sample has been cooled.

Since spontaneous emission cannot be eliminated, we have chosen to demonstrate this effect using an atomic transition with a large ω_r and relatively long τ. We use the He $2^3S \rightarrow 3^3P$ transition at $\lambda = 389$ nm, where $\omega_r = 2\pi \times 330$ kHz so that $t_c \approx 380$ ns. Since $\tau \approx 106$ ns and the time averaged excited state population is $\sim$0.4 [13], the average spontaneous emission time is $t_{SE} \approx 260$ ns. Thus, we expect an average of $\lesssim 1.5$ SE events during time t_c.

Our experiment was performed on a beam of He atoms initially excited to the 2^3S state by a continuous flow, dc-discharge source, cooled with liquid N_2 to produce an average longitudinal beam velocity of $\sim$1050 m/s [14,15]. Our one-dimensional cooling axis is oriented perpendicular to the axis of this diverging atomic beam and narrows its transverse velocity distribution, thereby producing partial collimation. We use the bichromatic force, implemented with two frequencies tuned to $\omega_a \pm \delta$ [see Fig. 2(a)].

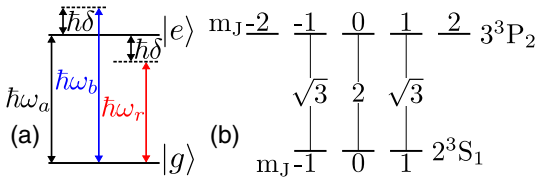

FIG. 2 (color online). Part (a) shows the two atomic levels and the detuning $\delta \gg \gamma$. Part (b) shows the $\Delta m = 0$ transitions driven by the linearly polarized light between the $J = 1$ and $J = 2$ He levels and their relative strengths.

The atomic beam emerges from the 500 μm diameter source aperture and crosses the bichromatic standing wave beams where it expands by $\approx \Delta v_B \times t_c = (\delta/16\omega_r)\lambda \approx 5\lambda$ for our parameters. Thus, the bichromatic force does not produce very much spatial spreading. The atomic beam exits the light field and then expands freely in the cooled transverse dimension during a 63 cm flight to the detector. Measurement of the spatial distribution downstream is readily converted to the transverse velocity distribution.

The He atoms are detected using a microchannel plate and phosphor screen to image their transverse spatial distribution. The screen is viewed by a video camera whose frames are stored at 30 Hz. The transverse spatial spread at the end of the 63 cm flight is very much larger than our 24 mm detector. Thus without any optical interaction, the detector sees a flat He distribution, but spatial variations in detector sensitivity produce a nonuniform camera image and such images are used to correct the data images.

The $\lambda = 389$ nm light for the optical standing waves is produced by a frequency-doubled, cw, narrow line width Ti:sapphire laser of wavelength 778 nm. This laser is frequency locked to better than γ with a stable cavity whose length is controlled by feedback from a saturated absorption spectroscopy signal. The signal is derived from an rf discharge cell of He at $\lambda = 389$ nm, but detuned from resonance by $-\delta$ with an acousto-optic modulator (AOM).

The frequency-doubled light passes through an AOM operated at 2δ and 50% diffraction efficiency to produce two beams at $\omega_\ell = \omega_a \pm \delta$. The two beams are recombined with a polarizing beam splitter (PBS) and coupled into a UV, polarization-maintaining, single-mode optical fiber, suitable for both polarizations, for spatial mode matching, and for transport to the vacuum system. After exiting this fiber, the two orthogonally polarized frequencies are separated by another PBS oriented at 45° to the orthogonal linear polarizations, resulting in two linearly polarized bichromatic beams (see Ref. [5]).

The bichromatic standing waves are formed by orienting these two beams (each having both frequencies $\omega_a \pm \delta$) to be counterpropagating and aligned transverse to the He beam. To ensure a short interaction time, the Gaussian beams of 400 μm waists (800 μm $1/e^2$ full width) were masked by adjustable slits that were imaged directly on the atomic beam to minimize diffraction effects. The peak Rabi frequencies varied by $< 10\%$ across the light field.

To assure the desired exact crossings at the points labeled "A" in Fig. 1(a), there are two constraints. One is total absence of coupling to other states as discussed above, and the other is that the light shifts must cause the dressed state eigenvalues to just meet as shown. These conditions are connected via the relative spatial phase of the standing waves as discussed in Ref. [7]. For our choice of this spatial phase = $\lambda/8$ [see Fig. 1(b)], the Rabi frequencies at the standing wave antinodes must satisfy $\Omega = \sqrt{3/2}\delta$.

We tune our laser light to the transition from the $J = 1$ ground state to the $J = 2$ excited state since tuning to the $J = 1$ or $J = 0$ excited states would preclude some of the atoms because of the selection rules. We choose linearly polarized light to excite $\Delta m_J = 0$ transitions as shown in Fig. 2(b) because the three allowed π transitions have roughly the same strengths, with $3J$ values and hence, Rabi frequencies in the ratio of $\sqrt{3}:2:\sqrt{3}$ for a fixed light intensity [16]. Any other polarization choice would result in larger differences among the Rabi frequencies. The unpolarized atomic beam could not be optically pumped upstream of the bichromatic interaction region because of space constraints.

Because of this unavoidable compromise on choosing the best value of Ω, we made measurements over a range of light intensities to find the optimum for the bichromatic force. We recorded video images of the transverse atomic spatial distribution as the laser power was varied using an adjustable neutral density filter at the output of the transport fiber. Each video frame of the phosphor screen at a given laser power is averaged vertically for smoothing (the force is horizontal), and then we make a three-dimensional composite plot of these averages for the various laser powers. We have a few dozen of these composites that take 2–3 minutes to record and one of these is shown in Fig. 3.

At low laser power, there is no measurable response of the atoms in the velocity range of the bichromatic force, but as the laser power is increased the effects of the bichromatic force emerge [see Fig. 3(a)]. Here, the darker purple represents reduced He intensity and lighter areas represent increased intensity, where the initial velocity distribution is flat and extends well beyond the detector limits shown here. An individual transverse velocity profile near $\Omega = 2\pi \times 36$ MHz is shown in Fig. 3(b).

It is clear from Fig. 3(b) that the atoms that began in the velocity range from -6 to $+2$ m/s are accelerated into the range from $+2$ to $+11$ m/s, whereas the atoms originally in that range are not accelerated, resulting in an increase in velocity space density. We note that the atoms are collected near the velocity limit of the force.

It is important to observe that this velocity change from -3 m/s to $+6$ m/s [dip to peak in Fig. 3(b)] of ~9 m/s

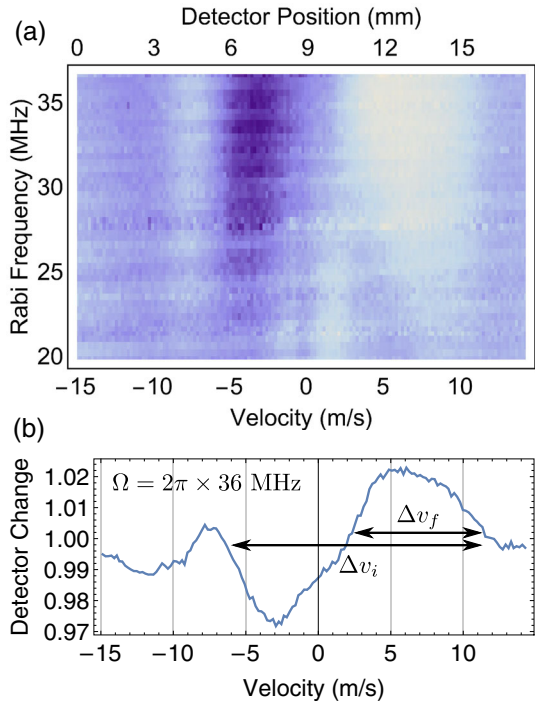

FIG. 3 (color online). Data taken with an optical slit width ≈230 μm, corresponding to interaction time of 220 ns $< t_{SE}$ for longitudinal velocity ≈1050 m/s. The detuning was $\delta = 2\pi \times 25$ MHz, corresponding to $\Delta v_B \approx 4.9$ m/s. In part (a), the dark regions represent reduced atomic intensity and the lighter regions increased intensity. The image has been corrected for detector inhomogeneity as discussed in the text. Part (b) shows a profile taken near the top of part (a) at $\Omega \approx 2\pi \times 36$ MHz. The initial (Δv_i) and final velocity widths (Δv_f) are indicated.

corresponds to ≈35 times the recoil velocity $\hbar k/M \approx 0.26$ m/s and is also $\sim\delta/k = 2\Delta v_B$. We emphasize that this is accomplished in an interaction time of only $(5/6)t_{SE}$, and note that this confirms that the observed forces derive almost purely from stimulated effects, i.e., the bichromatic force without SE.

Our dressed state model predicts that 25% of the atoms will experience a force opposite to that of the other 75% in the desired direction. This occurs because atoms enter the light field at different positions along the standing waves (horizontal axis of Fig. 1), and on a given manifold have a 3∶1 probability of seeing a positive as opposed to a negative slope (force). Figure 3(b) shows a smaller peak near −8 m/s that we attribute to this effect, and further corroborates the applicability of our model.

We have done simulations of this experiment that are based upon complete numerical solution of the optical Bloch equations. The results compare quite well with our data, and will be presented in some detail in a later publication.

There are a few separate effects that degrade the appearance of our cooled velocity distribution. First, time-of-flight (TOF) measurements of the longitudinal atomic velocity distribution show that its half height points are at ≈700 and 1250 m/s, corresponding to a spread of about half of the 1050 m/s center. Thus, atoms with the same transverse velocities are deflected by angles ranging over a factor of > 2 contributing to spatial spread at the detector. Our assignments of transverse velocity widths are therefore upper limits to the true He distribution. Deconvolving this longitudinal velocity distribution from the peak shown in Fig. 3(b) near $v = 6$ m/s would be fruitless because of its large width. However, there is no effect on the width of the dip near −3 m/s because there are no atoms left there as discussed below. We performed experiments with TOF resolution but their low resolution and lower S/N showed no improvement.

Next, our detector is sensitive to VUV light and other background emitted from the He source so that there is only a 5% peak-to-peak range of the profile in Fig. 3(b). Independent measurements of the total atom flux have shown that this represents very nearly all the atoms. Also, as discussed previously, the applied standing waves have different Rabi frequencies for the three transitions shown in Fig. 2(b). This means that over the range of laser intensities used for the data of Fig. 3, there is no point at which all atoms have the ideal value. For a truly two-level atom, this could be optimized providing better results.

We have demonstrated the very controversial notion of laser cooling in the absence of SE. The width of our final velocity distribution has been reduced by ×2 in the region of interest, thereby reducing the temperature by ×4. In addition, it is a compression of occupied phase space volume because the spatial expansion of the atomic sample is limited by the short interaction time to $\sim 5\lambda$ and the original sample size is 500 μm $> 10^3\lambda$.

Because the light field and the atoms must be considered as parts of the complete system under study, this process does not violate the dissipation requirements of Ref. [17]. The dissipation occurs when the light beams leave the system and are absorbed by the environment [11] (the system is open, not closed). Thus, there is indeed the required dissipation.

In conclusion, we have demonstrated cooling and phase space compression of an atomic sample without SE using a two-frequency laser field. This bichromatic force is the simplest extension from single-frequency forces, although there have been studies of other forces from polychromatic fields [10,13]. The potential for these polychromatic forces to cool should allow the extension of laser cooling to systems without closed cycling transitions, such as molecules.

C. C. and B. A. are supported by Department of Education through GAANN program. C C., B. A., and H. M. were supported by the Office of Naval Research. We thank Xiang Hua for help with the numerical simulations and Martin G. Cohen for careful reading of the manuscript.

*Corresponding author.
harold.metcalf@stonybrook.edu

[1] W. D. Phillips and H. Metcalf, Phys. Rev. Lett. **48**, 596 (1982).
[2] J. V. Prodan, W. D. Phillips, and H. Metcalf, Phys. Rev. Lett. **49**, 1149 (1982).
[3] J. Dalibard and C. Cohen-Tannoudji, J. Opt. Soc. Am. B **2**, 1707 (1985).
[4] H. Metcalf and P. van der Straten, *Laser Cooling and Trapping* (Springer Verlag, New York, 1999).
[5] J. Söding, R. Grimm, Y. B. Ovchinnikov, P. Bouyer, and C. Salomon, Phys. Rev. Lett. **78**, 1420 (1997).
[6] M. T. Cashen and H. Metcalf, Phys. Rev. A **63**, 025406 (2001).
[7] L. Yatsenko and H. Metcalf, Phys. Rev. A **70**, 063402 (2004).
[8] T. Lu, X. Miao, and H. Metcalf, Phys. Rev. A **71**, 061405(R) (2005).
[9] X. Miao, E. Wertz, M. G. Cohen, and H. Metcalf, Phys. Rev. A **75**, 011402 (2007).
[10] D. Stack, J. Elgin, P. M. Anisimov, and H. Metcalf, Phys. Rev. A **84**, 013420 (2011).
[11] H. Metcalf, Phys. Rev. A **77**, 061401(R) (2008).
[12] R. Grimm, J. Söding, and Y. Ovchinnikov, Opt. Lett. **19**, 658 (1994).
[13] S. E. Galica, L. Aldridge, and E. E. Eyler, Phys. Rev. A **88**, 043418 (2013).
[14] J. Kawanaka, M. Hagiuda, K. Shimizu, F. Shimizu, and H. Takuma, Appl. Phys. B **56**, 21 (1993).
[15] H. Mastwijk, Ph.D. thesis, Utrecht University, 1997.
[16] M. A. Chieda and E. E. Eyler, Phys. Rev. A **84**, 063401 (2011).
[17] W. Ketterle and D. E. Pritchard, Phys. Rev. A **46**, 4051 (1992).